Wheat Germ Extract Decreases Glucose Uptake and RNA Ribose Formation but Increases Fatty Acid Synthesis in MIA Pancreatic Adenocarcinoma Cells

László G. Boros, *Károly Lapis, *Béla Szende, †Rita Tömösközi-Farkas, ‡Ádám Balogh,
§Joan Boren, §Silvia Marin, §Marta Cascante, and ‖Máté Hidvégi

*UCLA School of Medicine, Harbor-UCLA Research and Education Institute, Torrance, California, U.S.A.; *First Institute of Pathology and Experimental Cancer Research, Semmelweis Medical University, Budapest, Hungary; †Central Food Research Institute, Budapest, Hungary; ‡Department of Surgery, Albert Szent-Gyorgyi Medical and Pharmaceutical Center, School of General Medicine, University of Szeged, Szeged, Hungary; §Department of Biochemistry and Molecular Biology, Institut d'Investigacions Biomediques August Pi i Sunyer, University of Barcelona, Barcelona, Spain; and ‖Department of Biochemistry and Food Technology, Technical University of Budapest and Biromedicina Company, Budapest, Hungary*

Summary: The fermented wheat germ extract with standardized benzoquinone composition has potent tumor propagation inhibitory properties. The authors show that this extract induces profound metabolic changes in cultured MIA pancreatic adenocarcinoma cells when the $[1,2-^{13}C_2]$glucose isotope is used as the single tracer with biologic gas chromatography–mass spectrometry. MIA cells treated with 0.1, 1, and 10 mg/mL wheat germ extract showed a dose-dependent decrease in cell glucose consumption, uptake of isotope into ribosomal RNA (2.4%, 9.4%, and 28.0%), and release of $^{13}CO_2$. Conversely, direct glucose oxidation and ribose recycling in the pentose cycle showed a dose-dependent increase of 1.2%, 20.7%, and 93.4%. The newly synthesized fraction of cell palmitate and the ^{13}C enrichment of acetyl units were also significantly increased

with all doses of wheat germ extract. The fermented wheat germ extract controls tumor propagation primarily by regulating glucose carbon redistribution between cell proliferation–related and cell differentiation–related macromolecules. Wheat germ extract treatment is likely associated with the phosphorylation and transcriptional regulation of metabolic enzymes that are involved in glucose carbon redistribution between cell proliferation–related structural and functional macromolecules (RNA, DNA) and the direct oxidative degradation of glucose, which have devastating consequences for the proliferation and survival of pancreatic adenocarcinoma cells in culture. **Key Words:** Pentose cycle—Ribose synthesis—Fermented wheat germ extract—Nonoxidative glucose metabolism—Cell proliferation—Avemar.

In his later life, the Hungarian Nobel laureate biochemist Albert Szent-Györgyi extensively studied various extracts of the wheat plant for their anticarcinogenic effects. More recently, continued efforts to purify and produce anticarcinogenic fractions of wheat germ led to the development of an industrial fermentation process, which includes the standardization of benzoquinone content for purity and quality control in wheat germ extract

(Avemar, Biomedicina Co., Budapest, Hungary). Avemar has a marked inhibitory effect on metastasis formation in tumor-bearing animals (1). The inhibitory effect of Avemar on metastasis formation is attributed to its immune-restorative properties (2), which result in decreased survival time of skin grafts after transplantation and reduced cell proliferation but enhanced apoptosis and antioxidant effects with no dose-limiting toxic effects in experimental and clinical studies (3,4). Avemar exerts a remarkable inhibitory effect on tumor metastasis formation after chemotherapy not only in experimental animals but also in clinically advanced human colorectal cancers (4). Avemar is being evaluated in extensive studies as a potential adjuvant therapeutic agent in an array of human cancers, including those of the breast, colon,

lung, and prostate, with promising results in coapplication with current chemotherapeutic methods.

Plant isoflavonoids and benzoquinones regulate tumor cell proliferation through various mechanisms. Genistein, the isoflavonoid of the soy plant, exerts noticeable tyrosine kinase (5) and protein kinase (6) inhibitory effects, which result in cell cycle arrest (7) and diminished angiogenesis (8). Many plant alkaloids counteract the growth-promoting effect of human growth factors, including transforming growth factor-β, through their signaling pathways, which include signal coupling to transcription factors (9,10). Because the invasive transformation of human tumor cells is characterized by increased glucose intake and nucleic acid synthesis through specific nonoxidative reactions of the pentose cycle (11), it is likely that the wheat germ extract Avemar decreases invasive transformation and metastasis formation by inhibiting glucose-dependent intermediate metabolic pathways. Because Avemar provides the basis for an effective supplemental treatment strategy for therapy-resistant human cancers, including that of the pancreas, we wanted to determine how Avemar regulates nucleic acid, amino acid, lipid synthesis, carbon dioxide release, and glucose oxidation in pancreatic adenocarcinoma cells. We accomplished this using biologic mass spectrometry of key metabolites formed from a uniquely labeled glucose molecule in tumor cell cultures in the presence of increasing doses of the wheat germ extract Avemar.

MATERIALS AND METHODS

Cell line, culture, and treatment

MIA pancreatic adenocarcinoma cells (American Type Culture Collection, Rockville, MD, U.S.A.) were grown in minimum essential medium in the presence of 10% fetal bovine serum, at 37°C in 95% air and 5% carbon dioxide. MIA cells were selected for the study because their metabolism has been investigated extensively using stable glucose isotopes and their metabolic phenotype changes have been determined in response to tumor growth–modulating agents (12–14). Using standard cell counting techniques, we established cultures with 6×10^7 MIA cells before Avemar treatment, which were treated with increasing 0.1-, 1-, and 10-mg/mL doses of Avemar for 72 hours. Avemar doses were selected for the study because the effective dose of Avemar-inhibiting tumor metastasis formation in clinical studies is 9 g/day and this dose is equivalent to 0.5 to 1 mg/mL plasma concentration in a patient (depending on body weight) (4). To compare glucose utilization rates,

ribose synthesis, lactate production, and glutamine oxidation, MIA cells were incubated in [1,2-$^{13}C_2$]glucose-containing media (180 mg/dL, 50% isotope enrichment). Media glucose and lactate levels were measured using a Cobas Mira chemistry analyzer (Roche, Basel, Switzerland). Glucose oxidation was measured by media $^{13}C/^{12}C$ ratios in released carbon dioxide using a Finnegan Delta-S ion ratio mass spectroscope (GC/C/IRMS). $^{13}CO_2$ release was used to estimate glucose carbon utilization through oxidation by the cell lines and expressed as atom percent excess (APE), which is the percentage of ^{13}C produced by the cultured cells above the background level in calibration standard samples (15).

Stable [1,2-$^{13}C_2$]D-glucose isotope was purchased with more than 99% purity and 99% isotope enrichment for each position (Isotec, Miamisburg, OH, U.S.A.). For isotope incubation and drug treatment studies, MIA pancreatic adenocarcinoma cells were seeded in T-75 tissue culture flasks. During the study, the cultures were supplied with 50% [1,2-$^{13}C_2$]glucose dissolved in otherwise glucose- and sodium pyruvate–free Dulbecco modified Eagle medium with 10% fetal bovine serum. The final glucose concentration was adjusted to 180 mg/dL. Glucose mass isotope analysis of the medium before cell incubation showed that the actual labeled glucose enrichment was 56% in the culture media, and this number was used in further calculations to determine the maximum labeled glucose enrichment in the molecules we studied. Singly labeled ribose molecules (*m1*) recovered from RNA on the first carbon position were used to measure the ribose molar fraction, which is produced by direct oxidation of glucose through the G6PD pathway. Doubly labeled ribose molecules (*m2*) on the first two carbon positions were used to measure the molar fraction produced by transketolase. Doubly labeled ribose molecules (*m2*) on the fourth and fifth carbon positions were used to measure the molar fraction produced by triose phosphate isomerase and transketolase. Isotopomers with three labels were used to estimate ribose production by combining recycled products of the G6PD reaction through the transketolase and transaldolase reactions. Isotopomers with four labels (*m4*) were used to estimate synthesis through transketolase and triose phosphate isomerase. The possible rearrangement of labels from glucose to ribose as detected by gas chromatography–mass spectrometry in MIA pancreatic adenocarcinoma cells has been shown in previous studies by our group (12,13).

RNA ribose was isolated by acid hydrolysis of cellular RNA after Trizol purification of cell extracts. Before acid hydrolysis, the messenger and ribosomal RNAs

(mRNA and rRNA) of tumor cells were separated using the Qiagen RNA purification kit (Qiagen, Valencia, CA, U.S.A.). The ribose fraction of each RNA species was purified using a tandem set of Dowex1/Dowex50 ion exchange column (Sigma Chemical, St. Louis, MO, U.S.A.). Ribose was derivatized to its aldonitrile acetate form using hydroxil amine in pyridine and acetic anhydrate. We monitored the ion cluster around the $m/z256$ (carbons 1 to 5 of ribose, chemical ionization, CI), $m/z217$ (carbons 3 to 5 of ribose) and $m/z242$ (carbons 1 to 4 of ribose, electron impact ionization) to identify molar enrichment and the positional distribution of ^{13}C label in ribose (13,14).

Lactate from the cell culture media (0.2 mL) was extracted by ethyl acetate after acidification with hydrochloric acid. Lactate was derivatized to its propylamine-HFB form and the $m/z328$ (carbons 1 to 3 of lactate, chemical ionization) was monitored for the detection of $m1$ (recycled lactate through the pentose cycle) and $m2$ (lactate produced by the Embden-Meyerhof-Parnas pathway) for the estimation of pentose cycle activity (12).

Glutamate in the culture medium was isolated using a 3 cm^3 Dowex-50 (Supelco, Bellefonte, PA, U.S.A.) (H+) column. Amino acids were eluted from the Dowex-50 column with 15 mL 2N ammonium hydroxide, and the solution was evaporated to dryness by blowing air. To further separate glutamate from glutamine, the amino acid mixture was passed through a 3-cm^3 Dowex-1 (acetate) column. Glutamine was washed with 10 mL water, and glutamate was collected with 15 mL 0.5 N acetic acid. The glutamate fraction from tissue culture medium was converted to its trifluoroacetyl butyl ester form (16,17). Under electron impact ionization conditions, ionization of trifluoroacetyl butyl ester–glutamate yields two fragments, $m/z198$ and $m/z152$, corresponding to C2-C5 and C2-C4 of glutamate. Glutamate labeled on the 4–5 carbon positions indicates pyruvate dehydrogenase activity, whereas glutamate labeled on the 2-3 carbon positions indicates pyruvate carboxylase activity for the entry of glucose carbons to the Szent-Györgyi-Krebs (TCA) cycle (14). The TCA cycle metabolite alpha-ketoglutarate is in equilibrium with glutamate, which is released by the cells into the medium. The $m2/m1$ ratio in glutamate is proportional to the activity of glucose oxidation because $^{13}CO_2$ is released from alpha-ketoglutarate during each completed cycle. TCA cycle anaplerotic flux is calculated based on the $m2/m1$ ratios of glutamate using the method of Leimer et al. (17). Anaplerosis refers to the reactions that allow the entry of carbon into the TCA cycle intermediate pools other than through citrate synthase. Any carbon that enters the cycle as acetyl-CoA is oxidized to carbon dioxide and water;

any carbon that enters the citric acid cycle through an anaplerotic pathway is not oxidized but must be discarded by some other route. Glutamate dehydrogenase is one possible route that provides equilibrium between alpha-ketoglutarate and glutamate, and some other reactions include pyruvate carboxylation, transamination reactions, and propionate carboxylation.

Fatty acids were extracted with saponification of the Trizol cell extract (Rockville, MD, U.S.A.) after removal of the RNA-containing supernatant. Cell debris was treated with 30% potassium hydroxide and 100% ethanol overnight, and the extraction was performed using petroleum ether. Fatty acids were converted to their methylated derivative using 0.5 N methanolic–hydrochloric acid. Palmitate was monitored at $m/z270$ and stearate at $m/z289$. The enrichment of acetyl units and the synthesis of the new lipid fraction in MIA cells in response to Avemar treatment were determined using the mass isotopomer distribution analysis approach of different isotopomers of palmitate and stearate, as reported previously (18).

Gas chromatography–mass spectrometry

Mass spectral data were obtained using the HP5973 mass selective detector connected to an HP6890 gas chromatograph (Hewlett Packard, Palo Alto, CA, U.S.A.). The settings are as follows: GC inlet, 230°C; transfer line, 280°C; MS source, 230°C; MS 1uad, 150°C. An HP-5 capillary column (30 m long, 250 μm wide, 0.25 μm film thickness) was used for glucose, ribose, glutamate, and lactate analysis. A Bpx70 column (25 m long, 220 μm wide, 0.25 μm film thickness; SGE Incorporated, Austin, TX, U.S.A.) was used for fatty acid analysis with specific temperature programming for each compound studied.

Data analysis and statistical methods

In vitro experiments were performed using three cultures each time for each treatment regimen. Mass spectral analyses were conducted by three independent automatic injections of 1-μL samples by the automatic sampler and accepted only if the standard sample deviation was less than 1% of the normalized peak intensity. Statistical analyses were performed using the parametric unpaired, two-tailed independent sample t test with 99% confidence intervals ($\mu \pm 2.58\sigma$), and $p < 0.01$ was chosen to indicate significant differences in glucose carbon metabolism in MIA pancreatic adenocarcinoma cells treated with increasing doses of Avemar.

RESULTS

We compared metabolic changes observed in control untreated cultures of MIA pancreatic adenocarcinoma

cells with cultures treated with increasing doses of Avemar. Figures 1 and 2 show glucose consumption and lactate production of MIA cell cultures. Avemar exerted a dose-dependent inhibitory effect on glucose consumption but had little effect on lactate production, indicating that Avemar targets glucose but not three-carbon metabolite transport in MIA pancreatic adenocarcinoma cells. The greatest 10-mg/mL Avemar treatment inhibited glucose uptake by approximately 50%, as shown in Figure 1.

Figures 3 and 4 show the ^{13}C content (known as Σmn) of rRNA and mRNA, respectively, in response to escalating doses of Avemar treatment. Increasing doses of Avemar decreased ribose synthesis from glucose in both RNA fractions in a dose-dependent manner. It is also apparent from the mass spectrometry data that rRNA and mRNA have high turnover rates in MIA pancreatic adenocarcinoma cells, because both RNA fractions rapidly reach the theoretical maximum ^{13}C enrichment of ribose, which cannot exceed the 56% ^{13}C enriched glucose in the media. As is evident, Avemar treatment dramatically affects the synthesis of the rRNA fraction, with rapid 2.4%, 9.4%, and 28% decreases in isotope uptake through the nonoxidative branch of the pentose cycle. The messenger RNA glucose isotope content is greater than that of rRNA and its isotope content is decreased less in response to Avemar treatment. These results indicate that both RNA fractions have high turnover rates in MIA pancreatic adenocarcinoma cells and that Ave-

FIG. 2. Lactate production of MIA pancreatic adenocarcinoma cells in response to increasing doses of fermented wheat germ extract (Avemar) treatment after 72 hours of culture. Lactate production (m*M*) was estimated by the difference in media lactate content between Avemar-treated and control cultures. MIA cell lactate production was not significantly affected by Avemar treatment, indicating that the compound has little direct cell toxicity (x + SD; n = 6).

mar strongly influences the formation of RNA ribose from glucose.

Pentose cycle activity compared with glycolysis showed rapid 1.2%, 20.7%, and 93.4% increases in MIA tumor cells after 3 days of Avemar treatment, as indicated by increasing $m1/m2$ ^{13}C ratios in lactate (Fig. 5). Increased pentose cycle activity compared with the glycolytic flux and direct oxidation of the first carbon of
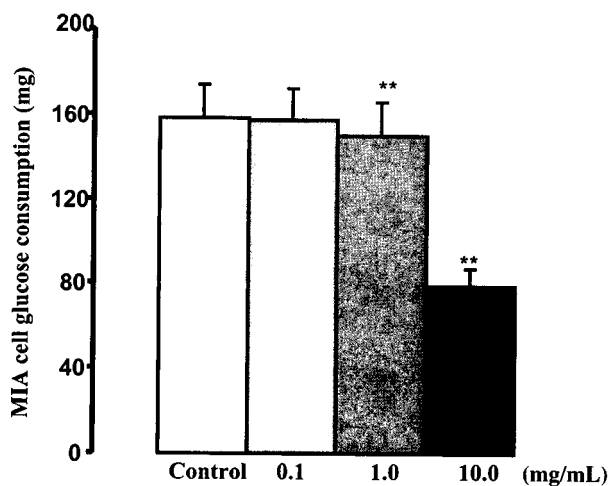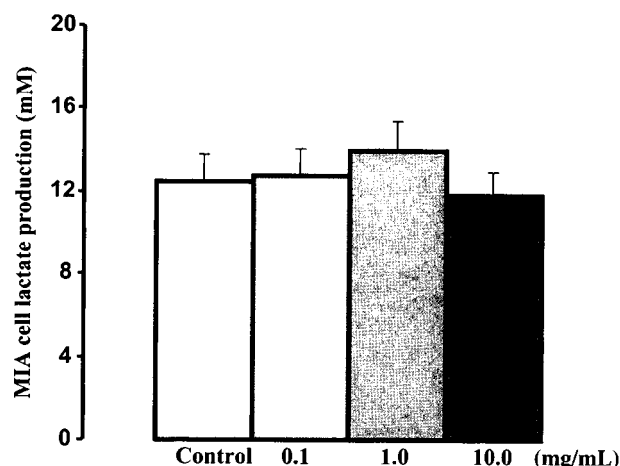

FIG. 1. Glucose consumption of MIA pancreatic adenocarcinoma cells in response to increasing doses of fermented wheat germ extract (Avemar) treatment after 72 hours of culture. Glucose consumption (measured in milligrams) was estimated by the difference in media glucose content between Avemar-treated and control cultures. MIA cell glucose consumption was significantly inhibited in the presence of either 1 mg/mL (*p < 0.05) or 10 mg/mL (**p < 0.01) Avemar (x + SD; n = 6).
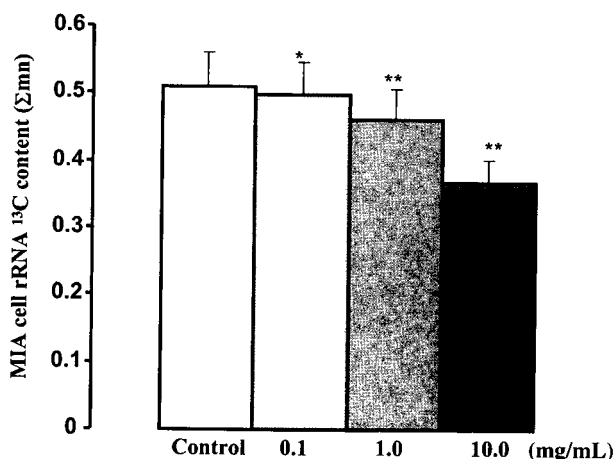

FIG. 3. Ribosomal RNA synthesis of MIA pancreatic adenocarcinoma cells in response to increasing doses of fermented wheat germ extract (Avemar) treatment after 72 hours of culture. Glucose carbon incorporation into ribose isolated from ribosomal RNA is expressed as molar enrichment (Σmn). The dose-dependent decrease in ^{13}C enrichment of rRNA after Avemar treatment indicates that ribosomal RNA synthesis is the primary site significantly affected by all doses of Avemar treatment with a maximum decrease of 29% after 10 mg/mL treatment (x + SD; n = 9; *p < 0.05, **p < 0.01).
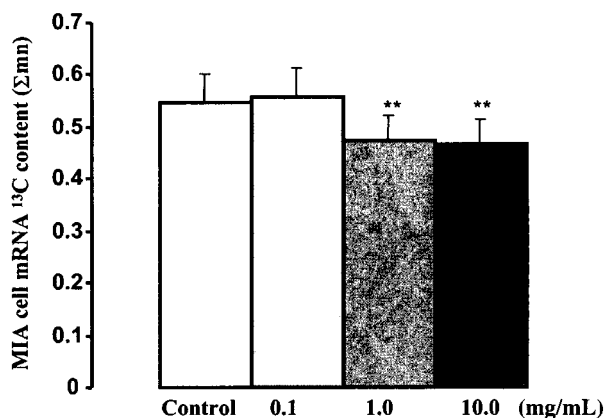
FIG. 4. Messenger RNA synthesis of MIA pancreatic adenocarcinoma cells in response to increasing doses of fermented wheat germ extract (Avemar) treatment after 72 hours of culture. Glucose carbon incorporation into ribose isolated from messenger RNA expressed as molar enrichment (Σmn). mRNA ^{13}C enrichment decreased by 15.8% and 16% after 1 and 10 mg/mL Avemar treatment, respectively (x + SD; $n = 9$; $*p < 0.05$, $**p < 0.01$).

glucose through G6PD indicates that Avemar has a substantial antioxidant effect on tumor cells by providing more reducing equivalent, NADP$^+$.

Glutamate mass isotopomers derived from [1,2-^{13}C$_2$]glucose indicate changes in the Szent-Gyorgyi-Krebs (TCA) cycle anaplerotic flux based on the equilibrium between glutamate and alpha-ketoglutarate. Glutamate stable isotope label rearrangement indicated a moderate decrease in TCA cycle anaplerotic flux, and only the maximum 10-mg/mL wheat germ extract dose

produced a significant change in the TCA cycle anaplerotic flux compared with glucose oxidation (Fig. 6). The decrease in ^{13}CO$_2$ release (Fig. 7) also indicated a decrease in cellular glucose uptake and oxidation.

The fraction of newly synthesized palmitate, the most abundant fatty acid membrane component, newly synthesized from glucose, was increased substantially after all doses of Avemar treatment (Fig. 8), and ^{13}C enrichment of acetyl units for fatty acid synthesis from glucose also showed a substantial increase after all doses of Avemar treatment (Fig. 9). This increase in fatty acid synthesis and the ^{13}C enrichment of acetyl units was not dose dependent, which can be explained by the decrease in glucose intake by tumor cells in response to increasing doses of Avemar treatment.

In conclusion, changes in metabolic activity indicate that Avemar treatment affects cell metabolism primarily by decreasing glucose uptake and nucleic acid ribose synthesis while increasing glucose oxidation through the oxidative reactions of the pentose cycle and fatty acid synthesis from glucose carbon. The effect of Avemar treatment on lactate production and TCA cycle anaplerotic flux compared with glucose oxidation is less prominent.

DISCUSSION

In this study, we investigated the metabolic response of cultured MIA pancreatic adenocarcinoma cells to wheat germ extract treatment, a potent plant derivative that inhibits tumor cell propagation. Use of the [1,2-^{13}C$_2$] stable glucose isotope tracer in metabolic investigations
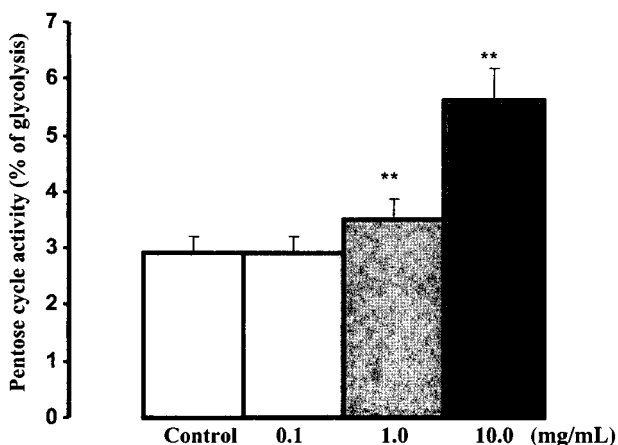

FIG. 5. Pentose cycle activity relative to glycolysis in MIA pancreatic adenocarcinoma cells in response to increasing doses of fermented wheat germ extract (Avemar) treatment after 72 hours of culture. Pentose cycle activity calculated by the $m1/m2$ ^{13}C ratios in lactate indicates that pentose cycle activity is approximately 2.9% of glycolysis without Avemar treatment. Increasing doses of Avemar treatment produce an increase in glucose oxidation and recycling relative to the glycolytic flux (x + SD; $n = 9$; $*p < 0.05$, $**p < 0.01$).
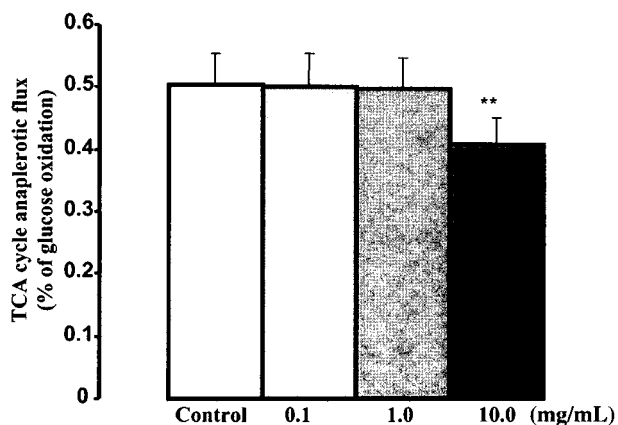

FIG. 6. TCA cycle anaplerotic flux in MIA pancreatic adenocarcinoma cells in response to increasing doses of fermented wheat germ extract (Avemar) treatment after 72 hours of culture. Changes in TCA cycle anaplerotic flux were less than that seen in glucose oxidation with increasing doses of Avemar. ^{13}C glucose enrichment of glutamate indicates an 18% decrease in TCA cycle anaplerotic flux after 10 mg/mL Avemar treatment (x + SD; $n = 9$; $*p < 0.05$, $**p < 0.01$).
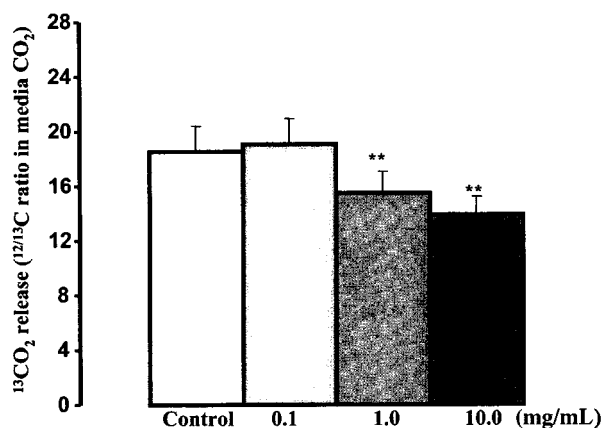
FIG. 7. $^{13}CO_2$ production by MIA pancreatic adenocarcinoma cells in response to increasing doses of fermented wheat germ extract (Avemar) treatment after 72 hours of culture. $^{13}CO_2$ release from [1,2-$^{13}C_2$]glucose exhibits a dose-dependent significant decrease after 1 and 10 mg/mL Avemar treatment (x + SD; $n = 9$; $*p < 0.05$, $**p < 0.01$).
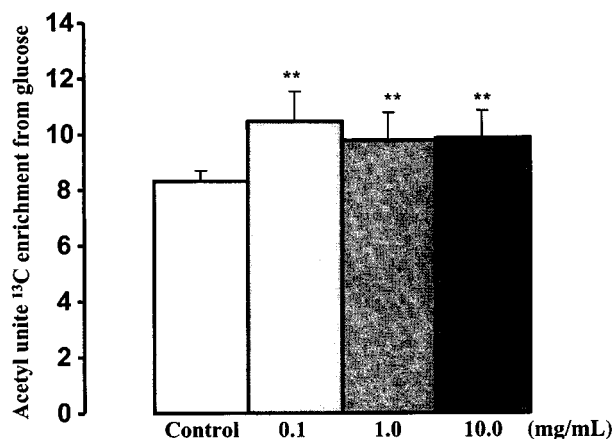

FIG. 9. Acetyl-CoA ^{13}C enrichment in MIA pancreatic adenocarcinoma cells in response to increasing doses of fermented wheat germ extract (Avemar) treatment after 72 hours of culture. ^{13}C enrichment of acetyl units used for lipid synthesis also shows a significant increase with all doses of Avemar treatment (x + SD; $n = 9$; $*p < 0.05$, $**p < 0.01$).

in cultures of human cells has enabled us to study a broad range of intracellular glucose intermediates and investigate their label distribution to determine carbon flow through various metabolic pathways simultaneously in response to this tumor growth-modifying agent. This approach has been successful in determining pentose cycle activity, the contribution of the two branches of the pentose cycle to nucleic acid ribose synthesis, TCA cycle activity, and lipid synthesis simultaneously in HepG2 and MIA pancreatic adenocarcinoma cells (12,13). It is evident from previous stable isotope studies that oncogenic processes primarily affect intermediate glucose
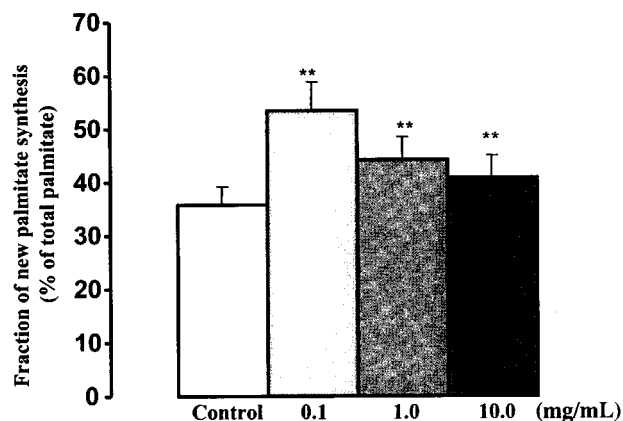

FIG. 8. Newly synthesized lipid fraction in MIA pancreatic adenocarcinoma cells in response to increasing doses of fermented wheat germ extract (Avemar) treatment after 72 hours of culture. The fraction of newly synthesized palmitate from glucose showed a significant increase at all doses of Avemar treatment, indicating a shift of glucose carbon utilization from nucleic acid synthesis to fatty acid synthesis in MIA pancreatic adenocarcinoma cells (x + SD; $n = 9$; $*p < 0.05$, $**p < 0.01$).

metabolism and the synthesis of macromolecules, which use glucose as a substrate. Transforming growth factor-β_2 recently was shown to induce profound metabolic changes in invasive lung epithelial carcinoma cells characterized by increased glucose use and nucleic acid ribose synthesis through the nonoxidative steps of the pentose cycle but decreased direct glucose oxidation and pentose cycle activity (11). Genistein, an isoflavonoid derived from soy, inhibits epidermal growth factor and transforming growth factor-β signaling in various tumors, and yet the underlying mechanism of its antiproliferative action in MIA cells is its ability to inhibit nucleic acid synthesis from glucose (12).

Data acquired in our study indicate that Avemar regulates tumor cell proliferation by altering the rate of glucose intake and the synthesis of nucleic acid ribose through the nonoxidative steps of the pentose cycle. This effect of Avemar is present most efficiently in the ribosomal RNA fraction of tumor cells. Because ribose is a close metabolite of glucose and ribosomal RNA is essential for de novo enzyme protein synthesis and cell proliferation, it is evident that inhibiting the formation of ribose from glucose to build ribosomal structures is one of the important underlying mechanisms by which Avemar regulates tumor cell growth.

Avemar also has remarkable effects on lipid synthesis and the oxidation of the first carbon of glucose through the oxidative steps of the pentose cycle. Avemar increases glucose oxidation dose dependently in the pentose cycle and therefore acts as an important agent in controlling oxidative stress and cell damage. The increase in *m1* lactate production cannot be observed in

rRNA or mRNA *m1* ribose, which strongly indicates that the oxidative steps of the pentose cycle play a limited role in the synthesis of ribose to build nucleic acid in tumor cells. This observation conflicts with previous models describing the pentose cycle (19) and confirms the new model of nonoxidative ribose synthesis established through metabolic control analysis (20).

The metabolic changes observed in MIA cells provide explanations for the clinically detected weight gain and slow disease progression of colorectal cancer in patients treated with Avemar (4). Increased pentose cycle activity leads to an increase in superoxide dismutase scavenger activity and lipid synthesis from glucose that promotes cell differentiation and protects against oxidative stress. Increased superoxide dismutase scavenger activity was recently reported in connection with low colorectal cancer development in carcinogen-treated rats consuming a wheat bran–enriched diet (21). Decreased glucose consumption of the tumors leads to a metabolic harmony with the host and weight gain in patients with even advanced cancers. As a result, Avemar-treated patients have improved tolerance for surgery, chemotherapy, or radiation therapy. The decrease in nucleic acid synthesis from glucose leads to a decrease in cell proliferation, which explains the slow progression of colorectal cancers and the increased survival rate compared with control tumor patients.

This effect of redistributing glucose carbon use from nonoxidative nucleic acid ribose synthesis to direct glucose oxidation and lipid synthesis is a novel mechanism of antiproliferative action. The findings reported in our studies indicate that the active compounds in fermented wheat germ extract share similar characteristics for regulating glucose metabolism to that of genistein. Avemar treatment is likely associated with the phosphorylation or transcriptional regulation of metabolic enzymes that are involved in reverting glucose carbons from cell proliferation–related structural and functional macromolecules (RNA, DNA) to direct oxidative degradation of glucose, which diminishes proliferation and survival of pancreatic adenocarcinoma cells in culture.

REFERENCES

1. Hidvegi M, Raso E, Tomoskozi-Farkas R, et al. Effect of Avemar and Avemar + vitamin C on tumor growth and metastasis in experimental animals. *Anticancer Res* 1998;18:2353–8.

2. Hidvegi M, Raso E, Tomoskozi-Farkas R, et al. Effect of MSC on the immune response of mice. *Immunopharmacology* 1999;41: 83–186.

3. Hidvegi M, Raso E, Tomoskozi-Farkas R, et al. MSC, a new benzoquinone-containing natural product with antimetastatic effect. *Cancer Biother Radiopharm* 1999;14:277–89.

4. Jakab F, Mayer A, Hoffmann A, Hidvegi M. First clinical data of a natural immunomodulator in colorectal cancer. *Hepatogastroenterology* 2000;47:393–5.

5. El-Zarruk AA, van den Berg HW. The anti-proliferative effects of tyrosine kinase inhibitors towards tamoxifen-sensitive and tamoxifen-resistant human breast cancer cell lines in relation to the expression of epidermal growth factor receptors (EGF-R) and the inhibition of EGF-R tyrosine kinase. *Cancer Lett* 1999;142: 185–93.

6. Waltron RT, Rozengurt E. Oxidative stress induces protein kinase D activation in intact cells involvement of Src and dependence on protein kinase C. *J Biol Chem* 2000;275:17114–21.

7. Lian F, Bhuiyan M, Li YW, et al. Genistein-induced G2-M arrest, p21WAF1 upregulation, and apoptosis in a non-small-cell lung cancer cell line. *Nutr Cancer* 1998;31:184–91.

8. Zhou JR, Gugger ET, Tanaka T, et al. Soybean phytochemicals inhibit the growth of transplantable human prostate carcinoma and tumor angiogenesis in mice. *J Nutr* 1999;129:1628–35.

9. Tacchini L, Dansi P, Matteucci E, et al. Hepatocyte growth factor signal coupling to various transcription factors depends on triggering of Met receptor and protein kinase transducers in human hepatoma cells HepG2. *Exp Cell Res* 2000;256:272–81.

10. Kim H, Peterson TG, Barnes S. Mechanisms of action of the soy isoflavone genistein: emerging role for its effects via transforming growth factor beta signaling pathways. *Am J Clin Nutr* 1998;68: 1418S–25S.

11. Boros LG, Torday JS, Lim S, et al. GF-β2 promotes glucose carbon incorporation into nucleic acid ribose through the nonoxidative pentose cycle in lung epithelial carcinoma cells. *Cancer Res* 2000;60:1183–5.

12. Boros LG, Bassilian S, Lim S, et al. Genistein inhibits nonoxidative ribose synthesis in MIA pancreatic adenocarcinoma cells: a new mechanism of controlling tumor growth. *Pancreas* 2000;22:1–7.

13. Lee W-NP, Boros LG, Puigjaner J, et al. Mass isotopomer study of the non-oxidative pathways of the pentose cycle with [1,2-$^{13}C_2$]glucose. *Am J Physiol* 1998;274:E843–51.

14. Boros LG, Puigjaner J, Cascante M, et al. Oxythiamine and dehydroepiandrosterone inhibit the non-oxidative synthesis of ribose and tumor cell proliferation. *Cancer Res* 1997;57:4242–8.

15. Kasho VN, Cheng S, Jensen DM, et al. Feasibility of analyzing [^{13}C]urea breath tests for Helicobacter pylori by gas chromatography-mass spectrometry in the selected ion monitoring mode. *Aliment Pharmacol Ther* 1996;10:985–95.

16. Lee W-NP, Edmond J, Bassilian S, Morrow JW. Mass isotopomer study of glutamine oxidation and synthesis in primary culture of astrocytes. *Dev Neurosci* 1996;18:469–77.

17. Leimer KR, Rice RH, Gehrke CW. Complete mass spectra of N-TAB esters of amino acids. *J Cromatogr* 1977;141:121–44.

18. Lee W-NP. Stable isotopes and mass isotopomer study of fatty acid and cholesterol synthesis. A review of the MIDA approach. *Adv Exp Med Biol* 1996;399:95–114.

19. Katz J, Rognstad R. The labeling of pentose phosphate from glucose-^{14}C and estimation of the rates of transaldolase, transketolase, the contribution of the pentose cycle, and ribose phosphate synthesis. *Biochemistry* 1967;6:2227–47.

20. Cascante M, Centelles JJ, Veech RL, et al. Role of thiamine (vitamin B₁) and transketolase in tumor cell proliferation. *Nutr Cancer* 2000;36:150–4.

21. Reddy BS, Hirose Y, Cohen LA, et al. Preventive potential of wheat bran fractions against experimental colon carcinogenesis: implications for human colon cancer prevention. *Cancer Res* 2000; 60:4792–7.